Preprint
UCRL-JC-150634

Simulation of Chamber Transport for Heavy-Ion Fusion

W.M. Sharp, D.A. Callahan Miller, M. Tabak, S.S. Yu, P.F. Peterson, D.V. Rose, R.C. Davidson, I.D. Kaganovich, E. Startsev, C.L. Olson

This article was submitted to: 19th IAEA Fusion Energy Conference, Lyon, France, 10/14-19/02

October 14, 2002

U.S. Department of Energy

Lawrence
Livermore
National
Laboratory

DISCLAIMER

Simulation of Chamber Transport for Heavy-Ion Fusion

W. M. Sharp 1), D. A. Callahan 1), M. Tabak 1), S. S. Yu 2), P. F. Peterson 3), D. V. Rose 4), D. R. Welch 4), R. C. Davidson 5), I. D. Kaganovich 5), E. Startsev 5), C. L. Olson 6)

1) Lawrence Livermore National Laboratory, Livermore, CA 94550, USA
2) Lawrence Berkeley National Laboratory, Berkeley, CA 94720, USA
3) University of California Berkeley, Berkeley, CA 94720, USA
4) Mission Research Corporation, Albuquerque, NM 87104, USA
5) Princeton Plasma Physics Laboratory, Princeton, NJ 08543
6) Sandia National Laboratory, Albuquerque, NM 87107

e-mail contact of main author: wmsharp@lbl.gov

Abstract. Beams for heavy-ion fusion (HIF) are expected to require substantial neutralization in a target chamber. Present targets call for higher beam currents and smaller focal spots than most earlier designs, leading to high space-charge fields. Collisional stripping by the background gas expected in the chamber further increases the beam charge. Simulations with no electron sources other than beam stripping and background-gas ionization show an acceptable focal spot only for high ion energies or for currents far below the values assumed in recent HIF power-plant scenarios. Much recent research has, therefore, focused on beam neutralization by electron sources that were neglected in earlier simulations, including emission from walls and the target, photoionization by radiation from the target, and pre-neutralization by a plasma generated along the beam path. The simulations summarized here indicate that these effects can significantly reduce the beam focal-spot size.

1. Introduction

During the last twenty-five years, the beam parameters favored for heavy-ion fusion (HIF) have changed dramatically. Early researchers conceived of using synchrotrons or radio-frequency accelerators to produced beams of multiply charged uranium ions with energies as high as 100 GeV[1]. At that energy, a total particle current on target of about 5 kA is needed to ignite a direct-drive target. When this current is divided among several beams, the near-vacuum transport of these beams 6-10 m to the center of a fusion chamber is virtually unaffected by the beam space charge. The US HIF program focused on induction accelerators after 1980, leading researchers to lower the beam energy by an order of magnitude [2], and the development of indirect-drive targets increased the required total energy several fold [3]. Nonetheless, ballistic transport of beams in the fusion chamber still appeared possible, provided the background-gas pressure could be kept less than a millitorr. During the 1990s, however, analyses of power-plant economics have strongly encouraged the use of lighter ions at higher currents, and the development of high-gain distributed-radiator targets has reduced the allowable beam-spot radius on the target. In addition, recent conceptual designs for HIF power plant use jets of molten salt to protect the fusion-chamber walls, substantially increasing the background-gas pressure. Taken together, these developments make it likely that beams in a practical HIF driver will require some form of neutralization during their final transport to the target.

In this paper, we use computer simulations to guide the choice of realistic parameters for a HIF driver. The numerical model is reviewed briefly in Section 2, and Section 3 discusses constraints on the choice of beam and chamber parameters. The results of a large number of simulations are summarized in Section 4, arriving at what we believe is a conservative but workable set of parameters.

2. Numerical Model

The principal computer code used for these chamber-transport simulations is LSP [4, 5], a multi-region and multi-species electromagnetic particle-in-cell code with a large palette of

particle models, boundary conditions, and physical interactions. The code models most physical processes expected in a fusion chamber, including electron emission from conducting walls, photoionization due to X rays from the heated target, and collisional ionization between the beam and background gas. Other processes, such as collisional scattering and recombination, are expected to be insignificant and are therefore neglected. A few aspects of the chamber environment, particularly the molten-salt jets and multiple ionization of the background gas, have not yet been incorporated into LSP simulations, but preliminary calculations indicate that these omissions do not seriously compromise the results. Although LSP can treat three-dimensional geometries and realistic initial conditions, the chamber-transport simulations here are axisymmetric and assume an idealized initial particle distribution. Further details of the numerical model are given in Ref. 6.

3. Parameters

Choosing parameters for a HIF driver conceptual design involves complicated tradeoffs. The target design determines total energy, the temporal variation of the input power, and the constraints on ion energy, incident angle, symmetry, and spot size. These requirements and constraints must be satisfied by choosing the number of beams and the ion species and energy, while trying to ensure efficient transport in the accelerator, successful final focus and chamber transport, effective shielding around the fusion chamber, and minimum overall cost. Chamber transport works most effectively with low-current beams of high-energy ions and large convergence angles, considerations that are best satisfied by using a large number of beams with heavier ions, such as bismuth (209 amu). However, the cost of induction accelerators increases roughly in proportion with ion energy, so economic considerations push toward the use of lighter ions, such as xenon (131 amu) at lower energy and higher current. Finally, designers of the fusion chamber would like to minimize both the number of beams and their convergence angle in order to minimize the escape of neutrons and debris. The parameters used in simulations here represent a compromise between these various conflicting demands.

The target chosen for the physics design here is a recent version of the distributed-radiator design introduced by Tabak and Callahan [7,8]. This indirect-drive target requires a total beam energy of 6.5-7 MJ, deposited with a time history approximating the dashed curve in Fig. 1a. About 3 MJ of this total must be delivered in "foot" pulses, beginning about 30 ns before the main pulses arrive, heating the hohlraum to about 100 eV and initiating the first shock wave in the capsule. The main pulses then deposit their energy in 8-10 ns, launching three more shock waves and igniting the fuel. To compensate for range-shortening as the target is heated, the energy of foot-pulse ions is 75% of the main-pulse ion energy. For successful ignition, 90-95% of the beam energy must be deposited in a 2.2-mm wide annulus on each end of the cylindrical target, and the incident angle of the beams must not exceed about 25^{o} from the target axis.

Since it is challenging to shape the final current profile of a beam [9] to match the input-power pattern shown in Fig. 1a, we choose instead to build up the pulse profile by overlapping beams of different current, energy, and duration, but each with approximately uniform current along its length. Such an arrangement is sketched in Fig. 1b, using 120 of five distinct types. The number of beams of each type must be an even multiple of eight or twelve to give adequate azimuthal symmetry on both ends of the target, and the total number is chosen so that the beam bundles entering each side of the chamber fit a nine-by-nine array of gaps between crisscrossed jets of molten salt. Corner beams are omitted to give the bundle approximate circular symmetry, and a square of nine gaps at the center is unused to allow target insertion and to reduce the differences between beam incident angles.

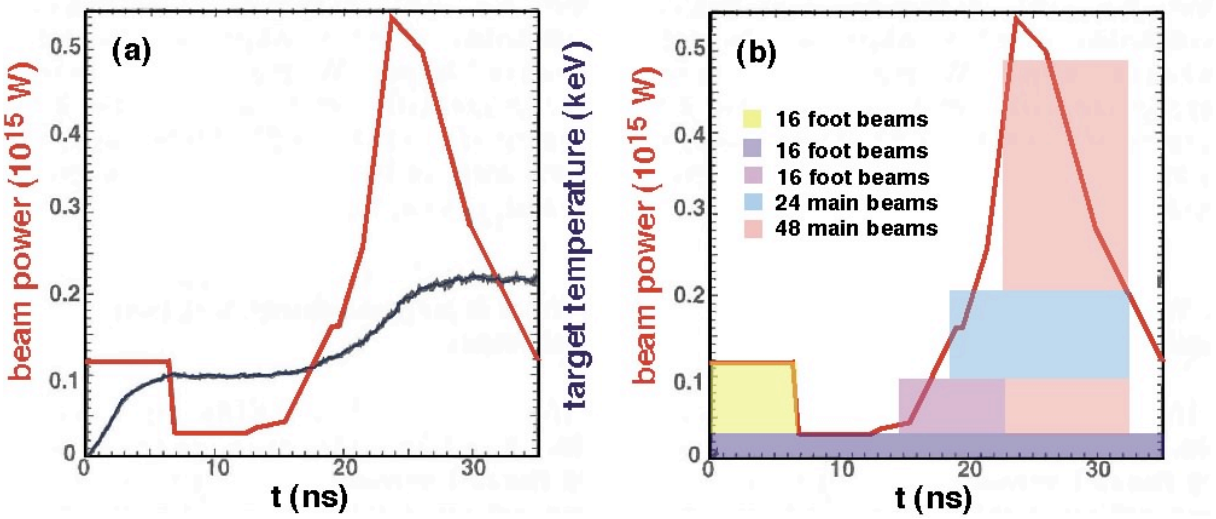

FIG. 1 (a) Typical time variation of input power and hohlraum temperature for a distributed-radiator target, and (b) a sketch showing how the power profile can be approximated by constant-current beams with different durations.

4. Results

The most challenging of the five basic beam formats to transport to the target are the initial short foot pulses that heat the hohlraum and the shorter of the two types of main pulse. The foot pulse is challenging because it must reach the target without additional neutralization from a photoionized plasma around the target, and the 9.3-ns main pulse is singled out because it has the highest current and generalized perveance [10]. The simulations reported here focus on these two pulse formats, and we use the results to determine the best choices for beam species and convergence angle.

4.1 Ballistic transport

We have made a series of runs to verify that near-ballistic transport is viable when the ion energy is sufficiently high. The low background-gas density needed to avoid beam stripping is inconsistent with a thick-liquid-wall chamber, so in these runs, we transport a 0.5 kA beam of singly charged 8-GeV lead ions a distance of 6 m through a 10^{12} cm^{-3} gas density, as is appropriate for a dry-wall or wetted-wall chamber [11]. For comparison, vacuum transport is also simulated.

In vacuum, the relatively low charge density and high rigidity of the beam lead to a focal spot that is less than twice the value expected from emittance alone, with 98% of the energy being deposited within a circle with a 2.2-mm radius. A weak halo is seen to form when background gas is present, but still 92% of the energy falls within the 2.2-mm spot. For vacuum transport, the only effect of photoionization by target X rays is stripping of beam ions as they approach the target, increasing the average charge state to nearly four and causing a 30% increase in emittance during the final 50 cm of transport. These changes decrease the charge deposition within a 2.2-mm spot to about 84%. This degradation, however, is not seen when the background gas is present, since neutralization by the photioionized gas offsets the additional stripping. For the case with background gas and photoionization, deposition within the nominal circle increases to 96% of the energy. We conclude that near-ballistic transport is possible even in the presence of photoionization and a realistic gas density. However, the higher ion energy makes this transport mode unattractive, both because of the accelerator increased cost and because target gain typically decreases for more energetic ions due to the larger mass needed to stop them.

4.2 Neutralized transport

For the higher perveance beams currently favored, space charge prevents a usable focal spot in the absence of external neutralization. The curves in Fig. 2a show the time variation of the beam root-mean-square (rms) radius at selected axial positions for a 3.2-kA pulse of 2.5 GeV Xe^{+} ions, corresponding to the 9.3-ns main pulse in Fig. 1b. The chamber background-gas density is 7 x 10^{12} cm^{-3}, as is appropriate for thick-liquid walls [12], and the gas density tapers off to zero in the final 50 cm of the beam port. For clarity, photoionization by target X rays has been turned off. The beam minimum radius, or "waist," occurs after 60 ns of transport, just after the beam has exited the beam port into the chamber, and by the time it reaches the nominal target location, about 100 ns, the radius is larger than the initial value. Although electron emission is allowed from beam port and chamber wall in this simulation, these electrons are ineffective at neutralizing the beam. Electrons from the beam-port wall are attracted by the beam space-charge field, gaining an energy that can exceed 10^{5} eV. Due to this thermal energy, many of these electrons escape the beam as it converges to the target. Emission from the target is likewise ineffective at neutralizing an impinging beam because the target surface quickly develops a large positive potential that curtails the further escape of electrons. Simulations with target emission show that the focal spot is virtually unaffected by the process.

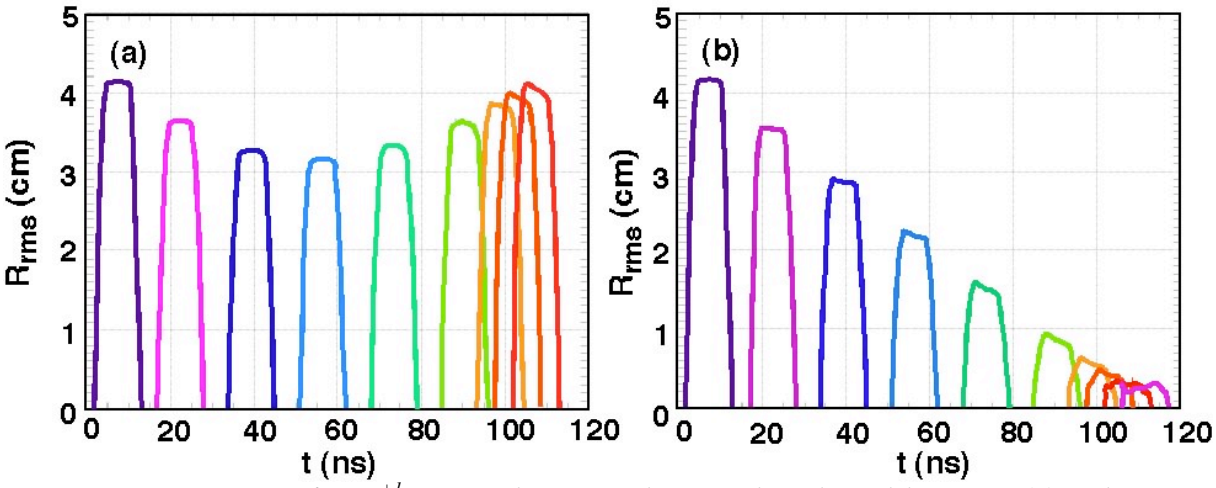

FIG. 2. Time variation of a Xe^{+1} main-pulse rms radius at selected axial locations (a) with no pre-neutralization and (b) with pre-neutralizing plasma placed near the ends of the beam port. Photoionzation has been turned off in these simulations.

Pre-neutralizing beams with highly ionized plasma near the chamber entry ports has been studied for a wide range of plasma, beam, and chamber parameters [13, 14, 15]. When the background-gas density is low enough that the characteristic length for ionization is comparable to the chamber radius, pre-neutralization is found to reduce significantly the beam spot size and emittance growth in the chamber. For the xenon main pulse in Fig. 1, adding a layer of fully ionized hydrogen plasma near each end of the 3-m beam port produces the greatly improved focal spot seen in Fig. 2b, with 81% of the beam energy falling within the nominal 2.2-mm spot. This focus is close to the target requirement, but the target physics must be analyzed carefully to ensure that the ions falling outside the intended annulus do not impair the radiation symmetry. The corresponding bismuth main pulse, with 2 kA and 4 GeV ions, focuses much better. The average rms waist radius is 1.8 mm, and 92% of the energy falls within the nominal spot. In a typical case, the focal-radius can be reduced about 10% by increasing the convergence angle from 10 mrad to 15 mrad. However, the larger entry ports

and the increased cone angle of the beam bundle would complicate design of the final-focus system and the neutron shielding. For these reasons, we choose to use the smaller convergence angle.

As foot pulses heat an indirect-drive HIF target, soft X rays emitted by the hohlraum photoionize the surrounding background gas. For reasonable gas densities, the resulting plasma is expected to improve neutralization near the target for main pulses and the late-arriving foot pulses. This additional neutralization is partly offset, however, by photostripping of the beam and by enhanced collisional stripping by the photoionized background gas. Main-pulse simulations including these photionization effects show a modest improvement in the beam spot. The average rms radius of the xenon main pulse drops from 3.1 to 2.4 mm at the waist, while for the corresponding bismuth pulse, it decreases from 1.9 to 1.5 mm, increasing the energy falling within a 2.2-mm radius spot to 94%. This focal spot easily satisfies the target requirement. These relatively small changes in radius mask larger changes in the transverse emittance and the beam charge state. For the bismuth case, the final emittance is 30% higher than without photoionization, and the average charge state increases from about 1.8 to nearly seven. These changes have little effect on the spot size, however, because they occur too close to the target to affect the beam transverse profile. For the current used here, magnetic self-pinching is negligible, although it is seen is simulations of beams having initial currents above 4 kA.

Using plasmas to pre-neutralize beams is particularly valuable for the reduced-current foot pulses that heat the target initially, since these beams must reach the target without additional neutralization from photoionization. For a 2.4-kA, 1.9-GeV Xe^{+1} foot pulse, corresponding to the first-arriving pulse in Fig. 1b, the rms radius at the waist varies between 2 mm at the head and 2.4 mm at the tail, with 84% of the beam falling within a 2.2-mm radius spot. The corresponding bismuth foot pulse, with 2-kA current and 3-GeV ion energy, again does substantially better, focusing to a 1.7-mm rms radius and depositing 92% of the energy within the nominal spot.

For all these cases, a plasma density of 3×10^{11} cm^{-3} is used, and each layer is 10 cm thick, plus 3-cm end regions with a parabolic density falloff. The results, however, are not sensitive to the plasma density, so long as the number of electrons in the volume swept out by the beam exceeds the total beam charge. Plasma pre-neutralization is enhanced by the proximity of a conducting wall because image charge on the pipe walls alters the plasma space-charge fields and makes it easier to remove electrons along the axis. Child-Langmuir electron emission from the walls, which is included in the simulations here, further improves beam neutralization by keeping the plasma quasi-neutral as electrons are extracted.

Although the residual space-charge potential after plasma neutralization is predicted to be independent of beam current [16], LSP simulations show some current sensitivity. As the current for a xenon main pulse is decreased from the nominal 3.2 kA to 0.4 kA, the waist radius decreases by roughly half. The cause of this change is anomalous emittance growth as a beam enters the first plasma layer. Electrons are drawn into the beam head as it approaches the plasma, producing a substantial positive current near the axis. The resulting nonlinear space-charge field leads to rapid growth in the beam emittance, particularly toward the beam tail. As expected, this effect increases with the beam current, but it is reduced substantially by increasing the scale length for density variation of either the beam or the plasma.

5. Conclusions

The beam and chamber parameters used here attempt to reconcile the conflicting demands of accelerator design, neutronics, final-focus, and targets. The final choice of 120 beams of

singly charged bismuth at 3-4 GeV is in no sense optimum, but the results to date indicate that such beams could be successfully transported to a fusion target and meet the requirements on spot size and deposition history. A crucial aspect of the successful transport is the use of low-density plasma to pre-neutralize beams before they enter the chamber. Some improvement in the focal spot results from increasing the nominal 10-mrad convergence angle to 15 mrad, but the larger entrance hole complicates chamber design and neutron shielding. Photoionization further improves the focal spot of main pulses by about 10% but, as expected, has a minimal effect on foot pulses.

In future simulations, we will add several features of chamber physics to the numerical model, particularly some representation of the molten-salt jets, and we will begin using more realistic distribution functions for the input beam. At the same time, the collaboration will continue between researchers working on the different accelerator subsystems to produce a workable physics design.

Acknowledgments

This work was performed under the auspices of the US Department of Energy by University of California Lawrence Livermore National Laboratory and Lawrence Berkeley National Laboratory under Contracts No. W-7405-ENG-48 and DE-AC-3-76SF00098.

References

[1] NUCKOLLS, J. H., "Target and Reactor Design," Proc. ERDA Summer Study of Heavy Ions for Inertial Fusion, Berkeley, CA, Lawrence Berkeley Laboratory Report LBL-5543 (1976), 1.
[2] HERRMANSFELDT, W. B., "Heavy Ion Accelerator Study Session," Proc. 1979 Heavy Ion Fusion Workshop, Berkeley, CA, Lawrence Berkeley Laboratory Report LBL-10301 (1980), 1.
[3] LINDL, J., Phys. Plasmas **2** (1995) 3933.
[4] HUGHES, T. P., *et al.*, Phys. Rev. ST Accel. Beams **2** (1999) 110401.
[5] WELCH, D. R., *et al*., Nucl. Instrum. Meth. Phys. Res A **464** (2001) 134.
[6] SHARP, W. M., *et al.,* "Modeling Chamber Transport for Heavy-Ion Fusion," Proc. 2002 IAEA Workshop on Targets and Chambers. (submitted).
[7] TABAK, M., CALLAHAN, D. A., Nucl. Instr. and Meth in Phys. Res. A **415** (1998) 75.
[8] CALLAHAN-MILLER, D. A., TABAK, M., Nucl. Fusion **39** (1999) 1547.
[9] SHARP, W. M., *et al.*, "Manipulation of High-Current Pulses for Heavy-Ion Fusion," AIP Conference Proceedings 391 (AIP Press, Woodbury, NY, 1997), 27.
[10] LAWSON, J. D., J. Electron. Control **5** (1958) 146.
[11] PENDERGRASS, J. H., Fusion Technol. **13** (1988) 290.
[12] OLANDER, D. R., *et al.*, Fusion Science Technol. **41** (2002) 141.
[13] ROSE, D. V., *et al.*, Nucl. Instr. and Meth in Phys. Res. A **464** (2001) 299.
[14] WELCH, D. R., *et al.*, Phys. Plasmas **9** (2002) 2344.
[15] SHARP, W. M., *et al*., "Chamber Transport of `Foot' Pulses for Heavy-Ion Fusion," Phys. Plasmas. (submitted).
[16] OLSON, C. L., Nucl. Instr. and Meth in Phys. Res. A **464** (2001) 118.